Registry No. Poly(styrene-*co*-HPB) (copolymer), 81273-49-6.

References and Notes

(1) Guillet, J. E.; Holden, D. A. "Developments in Polymer Photochemistry"; Allen, N. S. Ed.; Applied Science Publishers; London, 1980; Vol. 1, pp 1–68.
(2) Klopffer, W. In "Organic Molecular Photophysics"; Birks, J. B., Ed.; Wiley: London, 1973.
(3) Johnson, G. E. *J. Chem. Phys.* **1975**, *62*, 4697.
(4) Rambles, G. In "Photophysics of Synthetic Polymers"; Phillips, D., Roberts, A. J., Eds.; The Royal Institution; Science Reviews Ltd.: Northwood, England, 1982; p 5.
(5) De Schryver, F. C.; Vandendriesche, J.; Toppet, S.; Demeyer, K.; Boens, N. *Macromolecules* **1982**, *15*, 406.
(6) De Schryver, F. C.; Demeyer, K.; Vander Auweraer, M.; Quanten, E. *Ann. N.Y. Acad. Sci.* **1981**, *366*, 93.
(7) Gupta, A.; Liang, R. H.; Moacanin, J.; Kliger, D.; Goldbeck, R.; Horwitz, D.; Miskowski, V. M. *Eur. Polym. J.* **1981**, *17*, 485.
(8) Fox, R. B.; Price, T. R.; Cozzens, R. F.; McDonald, J. R. *J. Chem. Phys.* **1972**, *57*, 532.
(9) David, C.; Piens, M.; Gueskens, G. *Eur. Polym. J.* **1973**, *9*, 533.
(10) Kauffman, H. F.; Weixelbaumer, W.-D.; Buerbaumer, J.; Schmoltner, A.-M.; Olaj, O. F. *Macromolecules* **1985**, *18*, 104.
(11) Fredrickson, G. H.; Frank, C. W. *Macromolecules* **1983**, *16*, 1198.
(12) Yokota, M.; Tanimoto, O. *J. Phys. Soc. Jpn.* **1967**, *22* (3), 779.
(13) Fredrickson, G. H.; Anderson, H. C.; Frank, C. W. *J. Chem. Phys.* **1983**, *79* (7), 3572.
(14) Swank, R. K.; Buck, W. L. *Phys. Rev.* **1953**, *91* (4), 927.
(15) Swank, R. K.; Phillips, H. B.; Buck, W. L.; Basile, L. J. *IRE Trans. Nucl. Sci.* **1958**, *3*, 183.
(16) Gelles, R.; Frank, C. W. *Macromolecules* **1983**, *16* (9), 1448.
(17) Amrani, F.; Hung, J. M.; Morawetz, H. *Macromolecules* **1980**, *13*, 649.
(18) Ishii, T.; Handa, T.; Matsumya, S. *Makromol. Chem.* **1977**, *178*, 2351.
(19) Phillips, D.; Roberts, A. J.; Rumbles, G.; Soutar, I. *Macromolecules* **1983**, *16*, 1597.
(20) Gupta, M. C.; Gupta, A. *Polym. Photochem.* **1983**, *3*, 211.
(21) Ito, S.; Yamamoto, M.; Nishijima, Y. *Polym. J. (Tokyo)* **1981**, *13* (8), 791.
(22) Gupta, M. C.; Gupta, A.; Kliger, D.; Horowitz, D. *Macromolecules* **1982**, *15*, 1372.
(23) MacCallum, J. R.; Rudkin, A. L. *Eur. Polym. J.* **1981**, *17*, 953.
(24) Phillips, D.; Robertss, A. J.; Soutar, I. *Macromolecules* **1983**, *16*, 1593.
(25) This delayed fluorescence is presumably due to triplet–triplet annihiliation, and will be reported in more detail later.
(26) Berlman, I. B. In "Energy Transfer Parameters of Aromatic Compounds"; Academic Press: New York, 1973; p 112.
(27) Gupta, A.; Scott, G. W.; Kliger, D.; Vogl, O. In "Polymer for Solar Energy Utilization"; Gebelein, C. G., Williams, D. J., Deanin, R. D., Eds.; American Chemical Society, Washington, DC, 1983; ACS Symp. Ser. No. 220, p 293.
(28) Pradellok, W.; Gupta, A.; Vogl, O. *J. Polym. Sci., Polym. Chem. Ed.* **1981**, *19*, 3307.
(29) Bennet, R. G. *J. Chem. Phys.* **1964**, *41* (10), 3037.
(30) Reference 26, p 68.
(31) Förster, Th. *Discuss. Faraday Soc.* **1959**, *27*, 7.
(32) Pratte, J. F.; Webber, S. E. *Macromolecules* **1984**, *17*, 2116.
(33) Huston, A. L.; Scott, G. W.; Gupta, A. *J. Chem. Phys.* **1982**, *76*, 4978.
(34) Woersher, G.; Goeller, G.; Kollat, P.; Stezowski, J. J.; Houser, M.; Klein, U. K. A.; Kramer, H. E. A. *J. Phys. Chem.* **1984**, *88*, 5594.
(35) Werner, T.; Woersuer, G.; Kramer, H. E. A. In "Photodegradation and Photostabilization of Coatings"; Pappas, S. P.; Winslow, F. H., Eds.; American Chemical Society, Washington, DC, 1981; ACS Symp. Ser. No. 151, pp 1–18.
(36) Evesque, P. *J. Phys. (Les Ulis, Fr.)* **1983**, *44*, 1217.
(37) Even, U.; Rademann, K.; Jortner, *J. Phys. Rev. Lett.* **1984**, *52*, 2164.
(38) Klafter, J.; Blumen, A. *J. Chem. Phys.* **1984**, *80*, 875.

Ordered Structure in Aqueous Polysaccharide. 5. Cooperative Order–Disorder Transition in Aqueous Schizophyllan†

Takashi Itou and Akio Teramoto*

Department of Macromolecular Science, Faculty of Science, Osaka University, Toyonaka, Osaka 560, Japan

Takasuke Matsuo and Hiroshi Suga

Department of Chemistry and Chemical Thermodynamics Laboratory, Faculty of Science, Osaka University, Toyonaka, Osaka 560, Japan.

Received September 4, 1985

ABSTRACT: Optical rotation and heat capacity measurements were made on aqueous solutions of schizophyllan, a triple-helical polysaccharide. The heat capacity data showed that aqueous schizophyllan, either isotropic or cholesteric, exhibited a sharp thermal transition located around 279 K, and the transition enthalpy per mole of the polysaccharide repeating unit (648.6 g) was (2.83 ± 0.1) kJ mol^{-1} in H_2O and 3.96 kJ mol^{-1} in D_2O. The corresponding change in optical rotation was observed in the same temperature range, indicating that both changes originated from some common molecular event, presumably an order–disorder transition in a relatively short range surrounding the triple helix of schizophyllan. The transition was found to occur cooperatively among the saccharide units on the helix between the ordered and disordered states, although it was not of the all-or-none type. It was concluded that at lower temperature side-chain glucose residues of schizophyllan, helped by the surrounding water molecules, form a well-organized structure developing over a large distance along the helix axis, which becomes disordered with increasing temperature in a highly cooperative manner.

Aqueous solutions of schizophyllan, a triple-helical polysaccharide, form a cholesteric mesophase at high concentration;[1-3] Figure 1 gives the chemical structure of schizophyllan. It was shown in our previous publication[4] that such cholesteric solutions underwent a thermal transition around 280 K, as revealed by sharp changes in optical rotation and cholesteric pitch with temperature. These changes were accompanied by endothermic DSC peaks in the same temperature range. It was suggested that this transition may be associated with solvation of schizophyllan triple helices with water followed by reori-

† Contribution No. 97 from the Chemical Thermodynamics Laboratory.

0024-9297/86/2219-1234$01.50/0

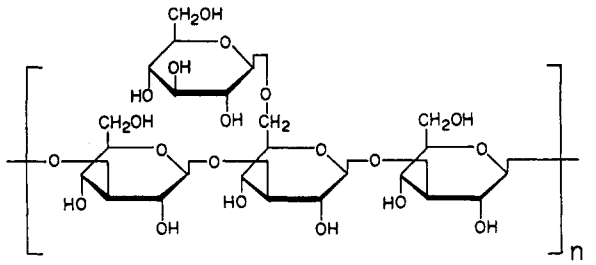

Figure 1. Repeating unit of schizophyllan.

Table I
Schizophyllan Samples Used

sample	$[\eta]^a/10^2$	$M_v/10^4$	N^b
J-4	0.320	8.4	130
J-3	0.464	10.5	162
R40	1.17	18.3	282
R-212	2.66	29.9	461
T-21-6	9.07	68.0	1049

[a] Intrinsic viscosities in water at 25 °C; units of $cm^3\ g^{-1}$. [b] N is the number of saccharide repeat units per triple helix.

entation of the solvated helices. However, the experimental data were not sufficient to work out a detailed molecular mechanism.

Recently, we found that isotropic solutions also exhibit a sharp change in optical rotation similar to those observed with the cholesteric solutions. This suggests that some molecular mechanism common to both isotropic and cholesteric solutions is responsible for this remarkable optical property. To our knowledge, such sharp changes in optical rotation are seldom seen in an isotropic solution unless they are associated with conformational transitions of the dissolved macromolecules such as helix–coil transitions in polypeptides.[5] The triple helix of schizophyllan has side-chain glucose residues that are regularly located outside its helical core and have a certain degree of freedom for rotational motion.[6] There is no structural requirement that the side chains themselves be organized into an ordered structure, since they are separated by more than 9 Å from one another so that no direct hydrogen bond or hydrophobic bond can be formed between them. However, it may be possible that the side chains are arranged in some ordered structure if they are helped by surrounding water molecules.

In this paper, we report measurements of optical rotation on isotropic solutions and of heat capacity on both isotropic and cholesteric solutions. Schizophyllan samples having different molecular weights were investigated to examine effects of molecular weight and concentration on the transition. The resulting data indicate that the transition is characteristic of a highly cooperative linear system, which appears to be consistent with the above possibility.

Experimental Section

Schizophyllan Samples. Sonicated schizophyllan supplied by Taito Co. Ltd. was fractionated according to the procedure described before,[7,8] and five fractions were chosen for the present study. The viscosity-average molecular weights M_v of the fractionated samples were determined from their intrinsic viscosities $[\eta]$ in water at 25 °C by using the $[\eta]$–M_w relationship established by Yanaki et al.[7] The results are summarized in Table I. According to Norisuye's analysis,[7,8] schizophyllan dissolves in water as a triple-stranded helix, which is intact and straight in this range of molecular weight. The polydispersity index M_z/M_w of the listed samples may be in the range between 1.2 and 1.5, as found with samples fractionated according to the same procedure.[7,8]

Aqueous solutions were prepared by mixing a weighed amount of a schizophyllan fraction with deionized water in a stoppered flask. The weight fraction w of polysaccharide was determined gravimetrically, and the mass concentration was computed from w along with the solution density data given elsewhere.[2] Part of the samples was lyophilized from D_2O solutions to make up D_2O solutions. D_2O (Wako) with a deuteration level greater than 99.75% was used.

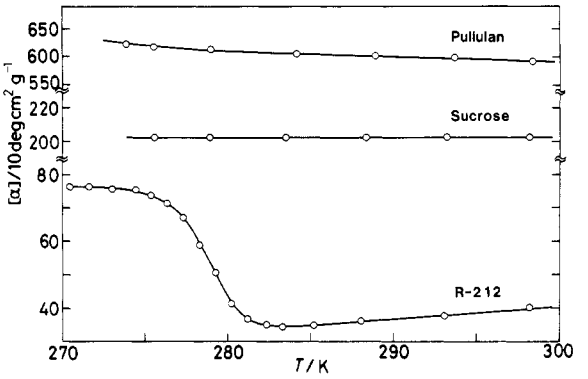

Figure 2. Temperature dependence of specific rotation $[\alpha]$ for light of wavelength 350 nm for aqueous solutions of schizophyllan R-212, sucrose, and pullulan; the number of repeating saccharide units per helix N = 461 for R-212.

Optical Rotation Measurements. Optical rotation measurements were made on a Jasco ORD/UV-5 spectropolarimeter with quartz cells of optical path length 10 cm for dilute solutions ($w \simeq 0.01$) and 2 cm for concentrated solutions ($w \simeq 0.08$). The temperature of the solution was measured by a thermocouple attached to the cell wall.

Heat Capacity Measurements. A renovated version[9] of the computerized adiabatic calorimeter[10] was used according to the experimental procedure established. The measurements were made between 272 and 300 K on four solutions with w = 0.07722 for sample R-212 and w = 0.07825, 0.1454, and 0.2116 for sample R40. Another solution of sample R-212 dissolved in D_2O with w = 0.07189 was examined between 277 and 303 K. Two or more series of measurements were repeated to ensure reproducibility of heat capacity data covering the necessary temperature range. In an additional experiment, the R40 solution with w = 0.1454 was rapidly cooled to liquid nitrogen temperature and kept for some time before the measurements at lower temperatures.

A known amount of a given solution weighing about 4 g was placed in the calorimeter cell and the cell was sealed, with helium as the conducting gas. In each cycle an accurately measured amount of energy was fed to the calorimeter cell and its temperature rise was measured; the temperature rise in each cycle was usually 0.5–1 K. The results were corrected for the heat capacity of the cell and helium gas. Temperature drift of the calorimeter due to nonideal adiabaticity was typically 2–5 mK h^{-1}. The heat leakage was corrected for by the rectilinear extrapolation of the temperature–time relation according to the standard practice of adiabatic calorimetry.[10] The correction for the vaporization of the solvent water into the vapor space in the cell was no greater than 0.015% of the net heat capacity of the solution at the highest temperature studied and neglected in the subsequent analysis. The quantities C_p thus determined refer to the polymer solutions saturated with helium and are equated to a good approximation to the heat capacities at the constant pressure p = 1 atm. The C_p values given below were calculated for the amount of the solution containing 1 mol of the polysaccharide repeating unit. The apparent partial molar heat capacity C_S of the polysaccharide repeating unit is computed from C_p by

$$C_S = C_p - C_w M_0(1 - w)/w \quad (1)$$

where C_w stands for the specific heat capacity of water and M_0 for the molar mass of the repeating unit; M_0 is taken to be 648.6 g mol^{-1} for schizophyllan.[7,8] The literature data[11,12] for C_w are used for the analysis to follow.

Results

Optical Rotation Data. Figure 2 shows the temperature dependence of specific rotation at 350 nm $[\alpha]$ for an isotropic solution of sample R-212. It is seen that $[\alpha]$ stays

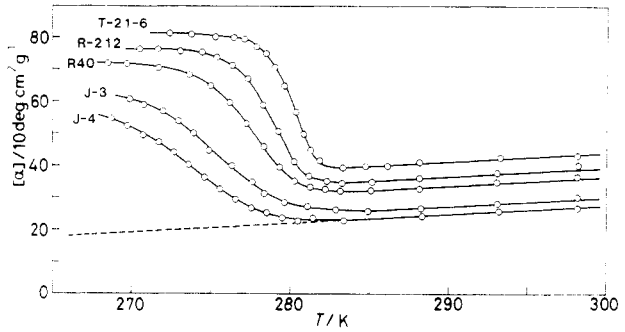

Figure 3. Plots of $[\alpha]$ at 350 nm vs. temperature for five schizophyllan samples ($w \simeq 0.01$) with N = 1049, 461, 282, 162, and 130 from top to bottom. The dashed line represents the base-line $[\alpha]_2$ (see text).

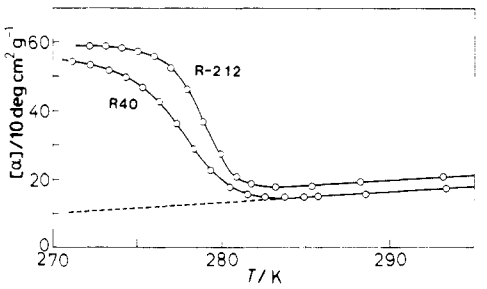

Figure 4. Plots of $[\alpha]$ vs. temperature for samples R40 and R-212 ($w \simeq 0.08$). N = 282 for R40 and 461 for R-212.

substantially constant at higher temperature but shows a sudden increase with lowering temperature around 280 K and tends to level off at a higher value. In this same temperature range were observed sharp changes in optical rotation and cholesteric pitch for cholesteric solutions of schizophyllan.[4] In contrast, $[\alpha]$ displays no such change for pullulan, which is shown to have no ordered conformation in water,[13-15] and for sucrose, indicating that this transition is not specific to glucose residues or polysaccharide chains in general. As will be shown below, it should be ascribed to the triple-helical conformation of schizophyllan but not to the cholesteric structure it forms.

Figure 3 shows $[\alpha]$ for dilute solutions of five samples with different molecular weights; the number N of repeating units per helix is used instead of molecular weight. As N is increased, the transition curve shifts to higher temperature and becomes sharper. Above the transition region all the curves are linear and almost parallel to one another. Figure 4 shows a similar trend in the $[\alpha]$ data for concentrated solutions with $w \simeq 0.08$. Precisely speaking, each transition curve continues to rise with decreasing temperature and does not appear to level off completely above 273 K; this trend is more conspicuous for lower molecular weight samples. When compared at the same molecular weight, the transition curve shifts slightly to higher temperature with increasing concentration, keeping its shape almost unchanged.

It was found that the dependence of $[\alpha]$ on wavelength λ of isotropic solutions was well represented by an equation of the Moffitt–Yang type with λ_0 = 150 nm

$$[\alpha] = \frac{\alpha_0 \lambda_0^2}{\lambda^2 - \lambda_0^2} + \beta_0 \left(\frac{\lambda_0^2}{\lambda^2 - \lambda_0^2} \right)^2 \qquad (2)$$

where α_0 and β_0 correspond to the Moffitt parameters a_0 and b_0, respectively, and are expressed in units of 10 deg cm^2 g^{-1}. The λ_0 value was determined by trial and error.

Panel a of Figure 5 shows plots of α_0 and β_0 for an isotropic solution of sample R-212 in the transition region.

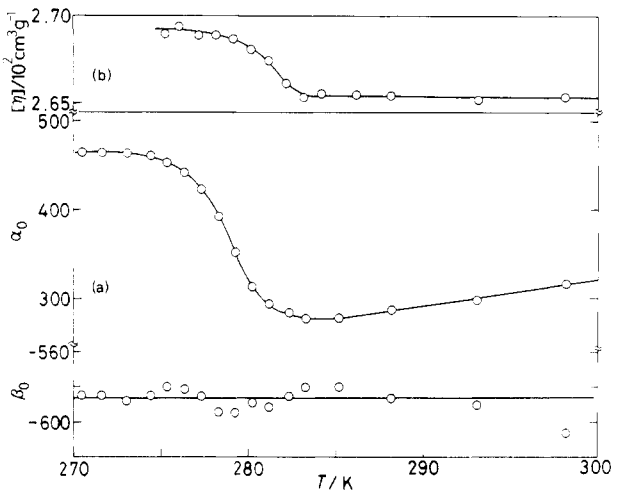

Figure 5. (a) Temperature dependence of the Moffitt parameters α_0 and β_0 for sample R-212. (b) Temperature dependence of intrinsic viscosity $[\eta]$ for sample R-212. N = 461.

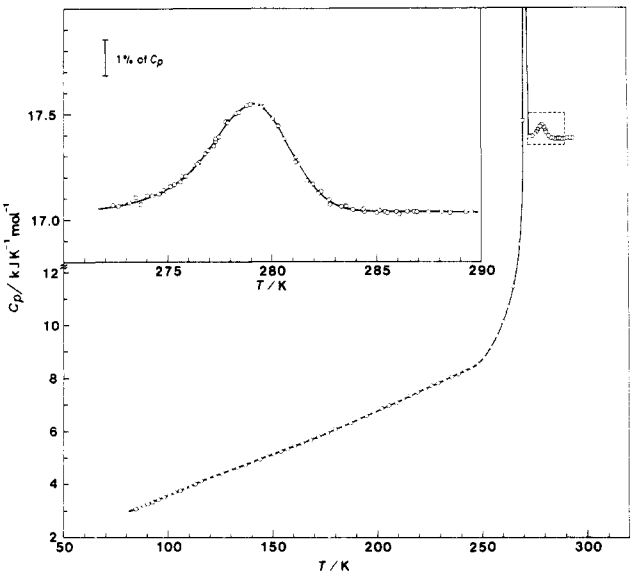

Figure 6. Heat capacity C_p of the solution with w = 0.1454 containing 1 mol of the saccharide repeating unit plotted against temperature for sample R40 with N = 282. The portion of the curve surrounded by the dashed line is enlarged in the insert.

It is seen that β_0 stays substantially constant at about −586 throughout the course of the transition but α_0 changes sharply in accordance with $[\alpha]$ (Figure 3); $-\beta_0$ is considerably smaller in dimethyl sulfoxide, in which schizophyllan is randomly coiled,[7,8] and virtually zero for pullulan, a random-coil polysaccharide.[13-15] It is also seen in panel b of Figure 5 that $[\eta]$ of sample R-212 increases only slightly with decreasing temperature in the transition region; $[\eta]$ is estimated to be 70 cm^3 g^{-1} in the random-coil state,[7,8] which is nearly 4 times as small as that in water. This implies that the triple-helical conformation of schizophyllan remains intact throughout the transition region as it is held firmly at 25 °C. Thus we conclude from these findings that the transition displayed by optical rotation is associated with the triple-helical conformation of schizophyllan in water but not specific to the cholesteric mesophase it forms.

Heat Capacity Data. All the numerical data from heat capacity measurements are summarized in the Supplementary Material. Figure 6 shows the C_p data for an aqueous solution of sample R40 with w = 0.1454. The heat capacity curve may be divided into three parts: a mo-

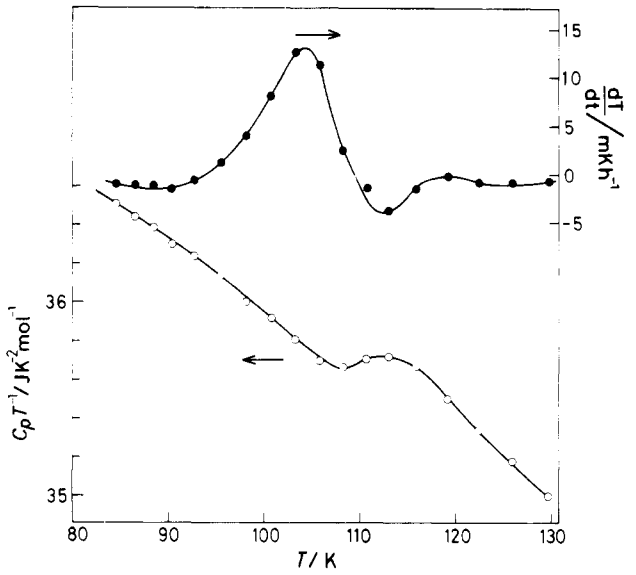

Figure 7. Plots of C_pT^{-1} and temperature drift dT/dt against temperature for the same solution shown in Figure 6.

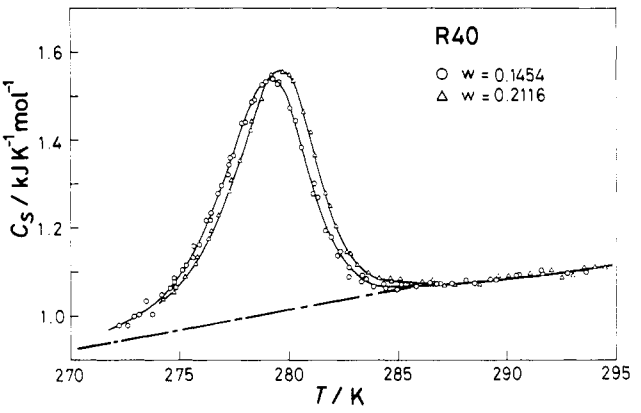

Figure 8. Apparent molar heat capacity C_S of the saccharide repeating unit for sample R40 in water: (○) isotropic solution (w = 0.1454); (△) cholesteric solution (w = 0.2116). The dash-dot line represents the base-line $C_B(T)$ (see text). N = 282 for R40.

notonous rise up to 250 K, a sharp peak centered about 273 K, which is ascribed to the fusion of the system, and a small endothermic peak at higher temperature, which is shown in an enlarged scale in the insert.

The first part is enlarged in Figure 7, where C_pT^{-1} is plotted along with the temperature drift, defined as the change in temperature in 1 h. There is an exothermic temperature drift between 93 and 110 K that is followed by an endothermic one centered around 112 K. The C_pT^{-1} vs. T curve has a small thermal anomaly in this temperature range. This type of thermal behavior is usually associated with an enthalpy relaxation phenomenon that appears in a glass transition region.[11] Indeed, this anomaly is quite similar to that in a rapidly cooled sample of ice (series 1) reported by Haida et al.[11] and may be related to the enthalpy relaxation in water occupying about 90% of the total volume of the solution.

As for the fusion part, the net energy input between 250 and 274 K was corrected for heat leakage (0.2%) and base-line heat capacity (3.0%) according to the standard procedure, yielding a value of 5713 J mol^{-1} for the molar enthalpy of fusion of ice. This value amounts to 95.1% of that for pure ice.[11] This may be taken to mean that as little as 4.9% of the total water contained in the solution remains unfrozen below the melting temperature. This finding is consistent with Hoeve's conclusion[16] that water

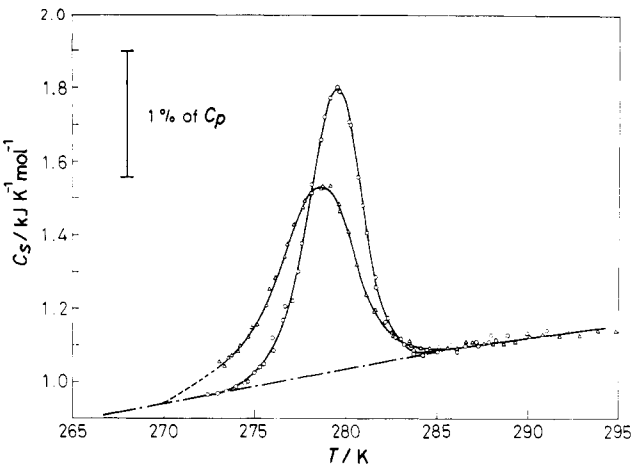

Figure 9. Plots of C_S vs. temperature for samples R40 (△) and R-212 (○) in water ($w \simeq 0.08$). N = 282 for R40 and 461 for R-212.

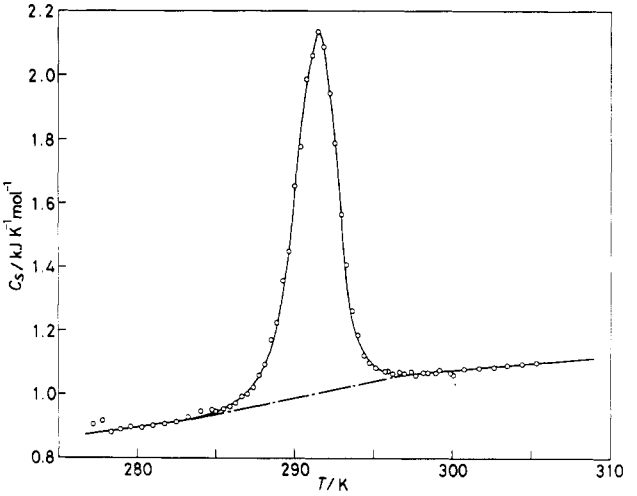

Figure 10. Plots of C_S vs. temperature for sample R-212 in D_2O. w = 0.07189.

absorbed in water-soluble polymers is essentially a single liquidlike phase in the thermodynamic sense.

The heat capacity curve has a well-defined endothermic peak located around 279 K, on which the following discussion will be specifically focused. Values of C_S were calculated by using these data according to eq 1, with the result shown in Figure 8. The C_S vs. T curve is characterized by a sharp peak centered near 279.2 K followed by a slightly rising plateau at higher temperature. This transition region agrees with the temperature range where sharp changes in optical rotation are observed for both isotropic and cholesteric solutions of schizophyllan.[4]

A cholesteric solution of sample R40 with w = 0.2116 was investigated similarly but only above the melting temperature. It is seen in Figure 8 that the C_S vs. T curve obtained is substantially the same as that for the above isotropic solution except that it is displaced by about 0.5 K to higher temperature from that of the latter. It should be noted that the plateau C_S values at higher temperature for the two solutions agree with each other within ±5 J K^{-1} mol^{-1}. This insensitivity of C_S to polymer concentration[17] is in conformity with the above conclusion that the observed transition is not associated with the liquid crystal structure of aqueous schizophyllan but with some properties of individual schizophyllan triple helices in water. It is important to note that C_S depends remarkably on polymer molecular weight in the transition region, as illustrated in Figure 9. In agreement with the [α] data shown in Figure 4, the transition appears at lower tem-

perature and is more gradual for the lower molecular weight sample than for the other.

Figure 10 shows C_S data for R-212 in D_2O. A sharp endothermic peak is seen at 291.5 K, about 12 K higher than that for the same sample in H_2O. This difference between the D_2O and H_2O solutions is noteworthy.

Discussion

Transition Curves and Transition Enthalpy. Let us assume that each saccharide repeating unit is either in the ordered state (1) or in the disordered state (2) and represent by f_N the fraction of units in the ordered state; one repeating unit consists of three main-chain glucose residues and one side-chain glucose residue.[7,8] Quantities associated with state i (i = 1, 2) are denoted by subscript i. $[\alpha]$ may be expressed by the sum of contributions $[\alpha]_1$ and $[\alpha]_2$ from the two states as

$$[\alpha] = f_N[\alpha]_1 + (1 - f_N)[\alpha]_2 \quad (3)$$

which is rearranged to give

$$[\alpha] - [\alpha]_2 = ([\alpha]_1 - [\alpha]_2)f_N \quad (4)$$

This equation allows f_N to be determined from $[\alpha]$ if values of $[\alpha]_1$ and $[\alpha]_2$ are known separately.

In a similar way, we have for the enthalpy H_r per mole of repeating unit

$$H_r = f_N H_1 + (1 - f_N)H_2 \quad (5)$$

where H_1 and H_2 stand for the enthalpies per mole of the corresponding units. Differentiating eq 5 with respect to T at constant pressure, we obtain

$$C_S = \partial H_r/\partial T = -\Delta H_r(\partial f_N/\partial T) + C_B(T) \quad (6)$$

with

$$\Delta H_r = H_2 - H_1 \quad (7)$$

$$C_B(T) = C_2(T) - (\partial \Delta H_r/\partial T)f_N \quad (8)$$

where ΔH_r is the transition enthalpy per mole of repeating unit, $C_2(T) = \partial H_2/\partial T$, and $C_B(T)$ is expected to be a slowly varying function of T and form the base line for C_S. Defining the transition heat capacity ΔC_S per mole of repeating unit by $\Delta C_S \equiv C_S - C_B(T)$, we get

$$\Delta C_S = -\Delta H_r(\partial f_N/\partial T) \quad (9)$$

If ΔH_r is assumed to be independent of T in the transition region, this equation may be integrated with respect to T to give

$$f_N(T) = -(\Delta H_r)^{-1}\int_{T_r}^{T} \Delta C_S \, dT \quad (10)$$

where T_r is a reference temperature taken above the transition region. $f_N(T)$ is unity at T below the transition region and zero at T_r.

In order to get f_N and ΔC_S from C_S and $[\alpha]$, it is necessary to know the base lines, $C_B(T)$, $C_2(T)$, $[\alpha]_1$, $[\alpha]_2$, etc., which have been determined as follows.

All the C_S vs. T curves in Figures 8 and 9 have well-developed linear portions at higher temperature, which are identified as $C_2(T)$. However, no such linear portion is seen at lower temperature, because data are not available below the transition region owing to crystallization; only the curve for sample R-212 has a short linear portion around 273 K. Thus it is difficult to determine $C_B(T)$ from these data alone.

It is seen in Figure 10 that the transition for R-212 in D_2O occurs about 14 K above the melting temperature of D_2O and the transition curve has well-developed linear portions on both sides of the transition region. Actually, the transition starts around 284 K and ends around 296 K, exhibiting a sharp peak at 291.5 K. Therefore we take the indicated dash–dot line as the base-line $C_B(T)$ for this solution. This base line is slightly more inclined than the linear portions.

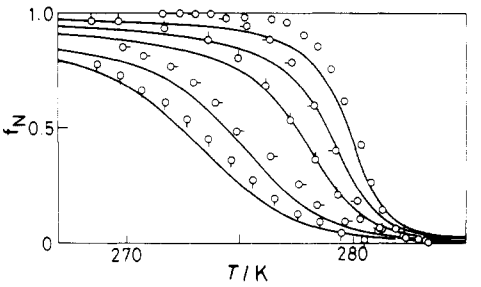

Figure 11. Temperature dependence of the fraction of the saccharide units in the ordered state. The values are deduced from the $[\alpha]$ data in Figure 3 for J-4 (○, pip down), J-3 (○, pip right), R40 (○, pip up), R-212 (○, pip left), and T-21-6 (○, no pip); solid lines, theoretical curves calculated by eq 14 for T_c^∞ = 280.2 K, ΔH_r = 3.7 kJ mol^{-1}, and $\sigma^{1/2}$ = 0.004 (see text).

The transition curve of R-212 in H_2O (Figure 9) resembles closely that in D_2O. Indeed it can be superimposed precisely on the latter when the peak height and temperature are made to agree with each other for the two solutions. This suggests that the H_2O solution of R-212 is still in a completely ordered state around 272 K. The base line for R-212 in Figure 9 (dash–dot line) has been determined from these considerations; the same base line is assumed for sample R40. The base line for R40 in Figure 8 has been determined from a similar consideration. The difference between the C_S vs. T curve and the base line gives ΔC_S at a given temperature.

It is seen in Figure 3 that for either sample $[\alpha]$ increases linearly with T above the transition region. This linear portion combined with its extension to lower temperature (dashed line) is taken as $[\alpha]_2$. It is evident from the above discussion that for higher molecular weight samples T-21-6 and R-212 the transition is yet to start around 271 K. We assume that $[\alpha]_1$ is independent of temperature and approximated by $[\alpha]$ values for these samples at sufficiently low temperature. Thus we take

$$[\alpha]_1 - [\alpha]_2(T = 268 \text{ K}) = 464 \text{ deg cm}^2 \text{ g}^{-1} \quad (11)$$

irrespective of molecular weight. Figure 11 shows plots of f_N for the dilute solutions calculated from $[\alpha]$ by using eq 4 and 11.

Panel a of Figure 12 shows the temperature dependence of ΔC_S for samples R40 and R-212 in H_2O. For sample R40 the transition is not completed with the temperature range examined, and the full transition curve has been obtained by extrapolation, as indicated by the dashed line. Values of ΔH_r were obtained by numerical integration according to eq 10, with ΔH_r assumed to be independent of T. The results are summarized in Table II, where T_c is the transition temperature at which ΔC_S becomes maximum and $\Delta S_r = \Delta H_r/T_c$. It is seen that in ordinary water ΔH_r is rather insensitive to molecular weight and concentration, being (2.83 ± 0.1) kJ mol^{-1} on the average. In heavy water both ΔH_r and ΔS_r are larger than the corresponding values in ordinary water.

The solid curves in panel b of Figure 12 represent the values of f_N calculated from ΔC_S according to eq 10. A good agreement of these values with those estimated from $[\alpha]$ data (circles and triangles) indicates that there is some common mechanism underlying these phenomena.

Type of Transition. The equilibrium constant K for the transition under consideration may be defined by

$$K = (1 - f_N)/f_N \quad (12)$$

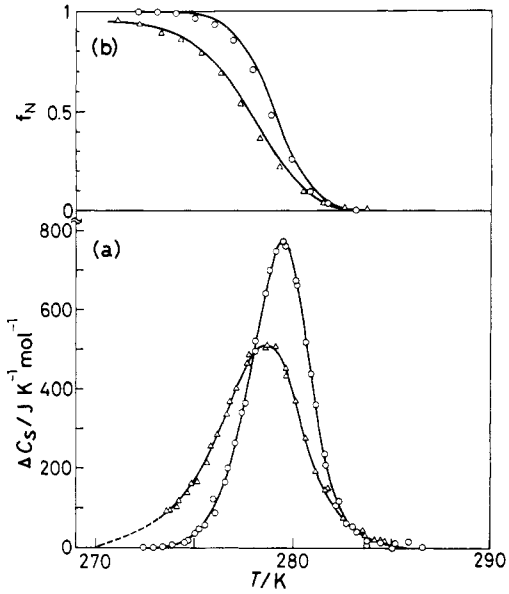

Figure 12. (a) Transition heat capacity ΔC_S plotted against temperature for R40 (△, w = 0.07825) and R-212 (○, w = 0.07722). (b) Plots of f_N vs. temperature for R40 and R-212; data points, values estimated from $[\alpha]$ in Figure 4; solid lines, values calculated from the ΔC_S vs. T in panel a. N = 282 for R40 and 461 for R-212.

Table II
Thermodynamic Quantities for the Order-Disorder Transition in Aqueous Schizophyllan[a]

sample	T_c, $T_{1/2}$	ΔH_r	ΔS_r	ΔH_{VH}	$\Delta H_{VH}N^{-1}$
R40					
w = 0.07825	278.7	2.81	10.1	428	1.52
w = 0.1454	279.2	2.75	9.8		
w = 0.2116	279.6	2.82	10.1		
R-212					
w = 0.07722	279.5	2.95	10.6	589	1.28
w = 0.07189[b]	291.5	3.96	13.6		

ORD Results ($w \simeq 0.01$)

sample	T_c, $T_{1/2}$	ΔH_{VH}	$\Delta H_{VH}N^{-1}$
J-4	273.0	264	2.03
J-3	275.0	315	1.94
R40	277.5	427	1.51
R-212	278.7	589	1.28
T-21-6	280.1	776	0.74

[a] Units are as follows: T_c and $T_{1/2}$, K; ΔH_r, ΔH_{VH}, and $\Delta H_{VH}N^{-1}$, kJ mol^{-1}; ΔS_r, J K^{-1} mol^{-1}. [b] Values in D_2O.

and the corresponding transition enthalpy ΔH_{VH} at $f_N = {}^1/_2$ is calculated from

$$\Delta H_{VH} = -4RT^2(\partial f_N/\partial T) \quad (13)$$

Values of ΔH_{VH} estimated from $[\alpha]$ data are given in Table II; $T_{1/2}$ is the temperature at which $f_N = {}^1/_2$.

If the transition is to occur in each unit independently of others, K should be independent of helix length, and so should be f_N, too. This possibility is ruled out because both C_S and $[\alpha]$ data show K to depend on molecular weight.

In a transition of the all-or-none type, all the units on a given helix are brought simultaneously from one state to another and no intermediate state exists. It then follows that ΔH_{VH} should be linearly related to helix length and approximately given by $\Delta H_{VH} \simeq N\Delta H_r$, where N is the number of repeating units per helix. It can be shown from the data in Table II that our transition is not of the all-or-none type. Finally we will discuss the possibility of a linear cooperative transition in aqueous schizophyllan in the following.

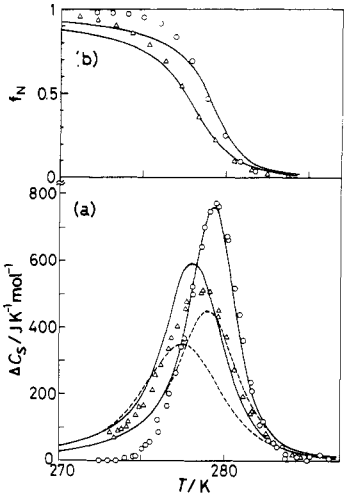

Figure 13. Comparison of the theoretical and experimental values for (a) ΔC_S and (b) f_N. Experimental values for R40 (△) and for R-212 (○). Theoretical values calculated for N = 282 and 461, T_c^∞ = 280.2 K and $\sigma^{1/2}$ = 0.004; dashed lines for ΔH_r = 3.0 kJ mol^{-1}, solid lines for ΔH_r = 3.7 kJ mol^{-1}.

Linear Cooperative Transition. It should be noted that the transition curves in $[\alpha]$ and C_S shown in Figures 3, 8, and 9 resemble closely those for thermal helix–coil transitions in polypeptides typical of linear cooperative systems.[5,18] Thus it is worthwhile to analyze the present data in terms of theories of helix–coil transitions in polypeptides.[5,19,20]

This resemblance between the two phenomena suggests that f_N correctly corresponds to helical content in the helix–coil transition. Thus we use the following approximate expression[5] for helical content as f_N:

$$f_N = f\left\{1 - 2[f(1-f)]^{1/2}/\beta + [1 + 2f^{1/2}(1-f)^{1/2}/\beta] \times \exp\left(-\frac{\beta}{[f(1-f)]^{1/2}}\right)\right\}\left\{1 + \left(\frac{f}{1-f}\right)\exp\left[-\frac{\beta}{[f(1-f)]^{1/2}}\right]\right\}^{-1} \quad (14)$$

f is the value of f_N for infinite N and $\beta = N\sigma^{1/2}$, with σ being the cooperativity parameter. f is related to ΔH_r by

$$f = (1/2)[1 + z(1 + z^2)^{-1/2}] \quad (15)$$

with

$$z = (\ln s)/2\sigma^{1/2} = \Delta H_r(1 - T/T_c^\infty)/(2\sigma^{1/2}RT) \quad (16)$$

where s is the familiar Zimm–Bragg parameter and T_c^∞ is the T_c (or $T_{1/2}$) for infinite N.

For a given solvent f_N is a known function of N with f and σ as the parameters depending on T. If data for f_N are available as a function of N, it is possible to test eq 14 by curve fitting.[5] Nagai[20] has given expressions for the average number g_N and the average length n_N of ordered sequences in a molecule as functions of N, s, and σ. No simple approximate expression is available for these quantities.

Values of ΔC_S were computed by eq 9 along with eq 14–16 with the experimental ΔH_r of 2.83 kJ mol^{-1} and for different $\sigma^{1/2}$ values. The dashed curves in panel a of Figure 13 represent the ΔC_S computed with this ΔH_r, T_c^∞ = 280.2 K, and $\sigma^{1/2}$ = 0.004. The computed and experimental curves are largely different in peak height. No better agreement between the two was achieved by using different σ values. In contrast, the solid curves repre-

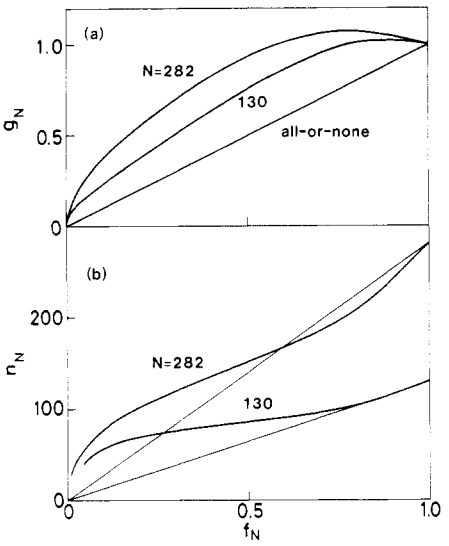

Figure 14. (a) Average number g_N of ordered sequences per helix as a function of f_N for $N = 282$ and 130. (b) Average length n_N of ordered sequences as a function of f_N. In panel a the indicated straight line refers to the transition of the all-or-none type.

senting the ΔC_S calculated with $\Delta H_r = 3.7$ kJ mol^{-1} satisfactorily reproduce the experimental data in the transition region. As seen in panel b, agreement between theory and experiment is also reasonably good for f_N in the transition region when the same set of parameters is used. It is seen in Figure 11 that this parameter set is also satisfactory for representing f_N for dilute solutions.[21] All these results may be taken to validate our analysis, giving evidence for a cooperative transition in aqueous schizophyllan, although we have no explanation at present to reconcile the disparity between the observed and assumed ΔH_r values.

The above σ value indicates that the transition is extremely cooperative when it is compared with those of polypeptides.[5,18] In the present case, an ordered sequence, once formed, tends to persist over a long distance on the helix. This situation may be well visualized by showing the average number g_N of ordered sequences and their average length n_N as functions of f_N.

Figure 14 shows how g_N and n_N calculated by Nagai's expressions vary with f_N for two molecular weights. For J-4 ($N = 130$) g_N is almost unity at f_N close to unity and n_N decreases in accordance with the decrease in f_N. At $f_N = 0.75$ g_N begins to decrease steadily with decreasing f_N, whereas n_N stays nearly constant at about 80 except at the final stage where $f_N < 0.1$. This calculation shows that there exists only one ordered sequence on a helix at the early stage of the transition. As the transition proceeds, the ordered sequence shrinks in accordance with the decrease in f_N, but completely disordered helices do not appear until f_N decreases to 0.75. Below this f_N the transition proceeds approximately in an all-or-none fashion; the system consists only of partially disordered helices and completely disordered ones and the fraction of the former determines f_N. The situation is similar in R40 ($N = 282$) but not so characteristic as in J-4. The possibility that a helix contains more than two ordered sequences is quite small unless N is very large.

Concluding Remarks

The experimental results and their analysis presented above have led us to conclude that there develops a well-organized structure about the side chains of the schizophyllan triple helix, which persists over a large distance along the helix axis and becomes disordered with increasing temperature in a highly cooperative manner. In the proposed model for the triple helix,[6] three polysaccharide chains constituting the helix have side-chain glucose residues at the same level along the helix axis with the identity period of 18.15 Å; the three glucose residues are directed outward from the helix core 120° apart. The nearest-neighbor residues on the same chain are located 18.15/2 Å apart along the helix axis and directed to the opposite sides of the helix. Thus any two side chains are separated by a distance longer than 18.15/2 Å, and no direct hydrogen bond or hydrophobic bond may be formed between them to stabilize some organized structure. However, it may be possible that the side chains may be organized in some way if they are helped by the surrounding water molecules; two water molecules suffice to fill the gap between the two nearest-neighbor side chains. The fact that the transition is affected remarkably by replacing H_2O with D_2O suggests an important role water molecules play in this transition. The detailed mechanism of the transition consistent with the conformation of the schizophyllan triple helix is yet to be elucidated.

Registry No. schizophyllan, 9050-67-3.

Supplementary Material Available: Experimental heat capacity data (7 pages). Ordering information is given on any current masthead page.

References and Notes

(1) Van, K.; Norisuye, T.; Teramoto, A. *Mol. Cryst. Liq. Cryst.* **1981**, *78*, 123.
(2) Van, K.; Teramoto, A. *Polym. J. (Tokyo)* **1982**, *14*, 999.
(3) Van, K.; Asakawa, T.; Teramoto, A. *Polym. J. (Tokyo)* **1984**, *16*, 65.
(4) Asakawa, T.; Van, K.; Teramoto, A. *Mol. Cryst. Liq. Cryst.* **1984**, *116*, 129 (part 4 of this series).
(5) Teramoto, A.; Fujita, H. *J. Macromol. Sci., Rev. Macromol. Chem.* **1976**, *C15*, 165. This review article summarizes important theoretical and experimental work on helix–coil transitions in polypeptides up to the mid-1970s.
(6) Takahashi, Y.; Kobatake, T.; Suzuki, H. *Macromolecules*, in preparation.
(7) Yanaki, T.; Norisuye, T.; Fujita, H. *Macromolecules* **1980**, *13*, 1462.
(8) Norisuye, T.; Yanaki, T.; Fujita, H. *J. Polym. Sci., Polym. Phys. Ed.* **1980**, *18*, 547.
(9) Matsuo, T.; Suga, H. *Thermochim. Acta* **1985**, *88*, 149.
(10) Kishimoto, K.; Suga, H.; Seki, S. *Bull. Chem. Soc. Jpn.* **1980**, *53*, 2748.
(11) Haida, O.; Matsuo, T.; Suga, H.; Seki, S. *J. Chem. Thermodyn.* **1974**, *6*, 815.
(12) Haida, O.; Suga, H.; Seki, S. *J. Glaciol.* **1979**, *22*, 155.
(13) Kato, T.; Okamoto, T.; Tokuya, T.; Takahashi, A. *Biopolymers* **1982**, *21*, 1623.
(14) Burton, B. A.; Brant, D. A. *Biopolymers* **1983**, *22*, 1769.
(15) Kawahara, K.; Ohta, K.; Miyamoto, H.; Nakamura, S. *Carbohydr. Polym.* **1984**, *4*, 335.
(16) Hoeve, C. A. J. In "Water in Polymers"; Rowland, S. P., Ed.; American Chemical Society: Washington, DC, 1980; ACS Symp. Ser. No. 127, p 135.
(17) This indicates that the partial molar heat capacity of the repeating unit may be closely approximated by C_S.
(18) Nakamoto, K.; Suga, H.; Seki, S.; Teramoto, A.; Norisuye, T.; Fujita, H. *Macromolecules* **1974**, *7*, 784.
(19) Zimm, B. H.; Bragg, J. K. *J. Chem. Phys.* **1959**, *31*, 526.
(20) Nagai, K. *J. Chem. Phys.* **1961**, *34*, 887.
(21) As seen in Figures 11 and 13, the agreement between theory and experiment is not satisfactory at low temperature. At present we have no reasonable explanation for this disagreement; inaccuracy in the base lines may be among the possible causes. With strict adherence to the triple helical conformation, N should be equated to $M_v/3M_0$. Then ΔH_r in eq 16 should be replaced by $3\Delta H_r$. This replacement gives rise to no change in our conclusion except that $\sigma^{1/2}$ is estimated 3 times as large as that given below.[22]
(22) Itou, T.; Teramoto, A.; Matsuo, T.; Suga, H. *Carbohydr. Res.*, in press.